# Structure of a Cys25→Ser mutant of human cathepsin S

**Johan P. Turkenburg,**[a]†
**Marieke B. A. C. Lamers,**[b]†‡
**A. Marek Brzozowski,**[a] **Lisa M.
Wright,**[a] **Roderick E. Hubbard,**[a]
**Simone L. Sturt**[b] **and David H.
Williams**[b]*‡

[a]York Structural Biology Laboratory, Chemistry
Department, University of York, Heslington,
York YO10 5DD, England, and [b]Medivir UK
Ltd, Peterhouse Technology Park, 100 Fulbourn
Road, Cambridge CB1 9PT, England

† These authors contributed equally to this
work.
‡ Present address: Millennium Pharmaceuticals
Ltd, Granta Park, Great Abington,
Cambridge CB1 6ET, England.

Correspondence e-mail:
david.williams@mpi.com

Cathepsin S (EC 3.4.22.27), a cysteine proteinase of the papain
superfamily, plays a critical role in the generation of a major
histocompatibility complex (MHC) class II restricted T-cell
response by antigen-presenting cells. Therefore, selective
inhibition of this enzyme may be useful in modulating class
II restricted T-cell responses in immune-related disorders such
as rheumatoid arthritis, multiple sclerosis and extrinsic
asthma. The three-dimensional structure at 2.2 Å resolution
of the active-site Cys25→Ser mutant presented here in an
unliganded state provides further insight useful for the design
of selective enzyme inhibitors.

## 1. Introduction

Cathepsin S is a single-chain cysteinyl proteinase of the papain
superfamily, highly stable at neutral or slightly acidic pH,
which was first isolated from bovine lymph nodes and spleen
(Kirschke *et al.*, 1986; Turnsek *et al.*, 1975). Subsequent
investigations have shown that expression of cathepsin S is
almost exclusively restricted to cells of lymphoid origin
(Kirschke *et al.*, 1989; Qian *et al.*, 1991; Shi *et al.*, 1994). Interest
has recently focused on cathepsin S and its role in immune-
system regulation.

Extracellular protein antigens are transported into antigen-
presenting cells *via* endocytosis or phagocytosis. These protein
antigens must be digested to small peptides, which are then
loaded onto the binding groove of major histocompatibility
complex (MHC) class II and presented for recognition by
CD4+ T lymphocytes (Germain & Margulies, 1993). Invariant
chain (Ii) is removed from $\alpha\beta$ MHC class II dimers by gradual
regulated cleavage of Ii by lysosomal proteinases (Cresswell,
1996; Newcomb & Cresswell, 1993; Roche & Cresswell, 1991)
including cathepsin S (Riese *et al.*, 1996, 1998). Indeed, mouse
gene knockout experiments have demonstrated that cathepsin
S deficiency results in a block in the processing of MHC class
II-associated invariant chain Ii, leading to markedly delayed
MHC class II peptide loading in B lymphocytes and dendritic
cells (Nakagawa *et al.*, 1999; Shi *et al.*, 1999). Moreover,
administration of the selective irreversible cathepsin S inhi-
bitor LHVS to mice results in accumulation of a Ii breakdown
product, attenuation of MHC class II peptide complex
formation and inhibition of antigen presentation (Riese *et al.*,
1998). For this reason, cathepsin S is considered a potential
target for autoimmune-disease therapy. However, inhibition
of the closely related family members cathepsin L and K could
lead to changes in skin and hair, and bone remodelling
(Gowen *et al.*, 1999; Hofbauer & Heufelder, 1999; Nakagawa

et al., 1998; Saftig et al., 1998), highlighting the need for inhibitor selectivity.

A homology model for cathepsin S was published in 1997 (Sumpter et al., 1997), followed by a 2.5 Å crystal structure of cathepsin S inhibited by a potent irreversible vinyl sulfone inhibitor, APC 2848 (McGrath et al., 1998). A single crystal, which took 18 months to grow, gave an incomplete data set and the structural model (which is not publicly available) lacked information necessary for drug design, including the position of water molecules, the cathepsin S-specific loop containing residues 58–61 (the numbering of the residues in the current structure is according to the human cathepsin S sequence) and the side chains of residues Val157 and Trp177. The mutant Cys25→Ser cathepsin S described here was amenable to rapid crystallogenesis and provided a full data set at 2.2 Å. The resulting model will be useful for the design of selective inhibitor molecules.

## 2. Experimental methods

The recombinant human cathepsin S enzymes for this study were expressed using baculovirus in Sf9 insect cells. The mutant Cys25→Ser enzyme was expressed at levels approaching 35 mg l$^{-1}$ as proenzyme with approximately half secreted and half kept inside the cells (Vernet et al., 1990). The protein was C-terminally hexahistidine tagged and was easily purified using metal–agarose column chromatography. Human cathepsin L was used to remove the pro-sequence from the mutant Cys25→Ser protein and the mature form of the mutant was totally inactive against the quenched fluorogenic cathepsin S peptide substrate Abz-Leu-Thr-Bal-Hyp-Tyr(NO$_2$)-Asp-NH$_2$.

Crystallization was performed by the hanging-drop vapour-diffusion method. Equal volumes of cathepsin S (Cys25→Ser) at 7 mg ml$^{-1}$, including the peptide Abz-Leu-Thr-Bal-Hyp-Tyr(NO$_2$)-Asp-NH$_2$ at 1 mM, and well solution were combined and placed over a well containing 20% 2-propanol, 20% PEG 2000 and 0.1 M sodium citrate pH 4.13. Rod-shaped crystals appeared after 10 d.

A crystal of cathepsin S (Cys25→Ser) with dimensions of $0.2 \times 0.1 \times 0.1$ mm was placed in a rayon loop and flash-cooled in a gaseous nitrogen stream at 120 K. Data were collected at 120 K using a MAR345 imaging-plate detector mounted on an RU-H3R Rigaku rotating-anode X-ray generator operating at 50 kV and 100 mA equipped with Osmic multilayers. The data were processed using the programs DENZO and SCALEPACK (Otwinowski & Minor, 1997). The crystals belong to the trigonal space group $P3_121$ or $P3_221$, with unit-cell parameters $a = b = 80.0$, $c = 61.5$ Å. Assuming one protein molecule in the asymmetric unit, the Matthews coefficient (Matthews, 1968) is 2.3 Å$^3$ Da$^{-1}$ corresponding to a solvent content of 46%. Data statistics are given in Table 1.

All further crystallographic calculations were performed using the CCP4 program suite (Collaborational Computational Project, Number 4, 1994). The cathepsin S (Cys25→Ser) structure was solved by molecular replacement

**Table 1**
Data collection and refinement statistics.

Values in parentheses are for the outer resolution shell.

| Space group | $P3_121$ |
| --- | --- |
| Resolution range (Å) | 20–2.2 (2.24–2.20) |
| $R_{sym}$ (%) | 7.5 (27.0) |
| Completeness (%) | 99.4 (98.8) |
| No. of observations | 39038 |
| No. of unique reflections | 11969 |
| $R_{free}$ test-set selection | Random |
| R value (working + test set) | 0.197 |
| R value (working) | 0.194 |
| $R_{free}$ | 0.251 |
| $R_{free}$ test-set size (%) | 5.0 |
| No. of reflections in $R_{free}$ test set | 597 |
| No. of non-H atoms used in refinement | 1857 |
| Average B value for non-H atoms (Å$^2$) | 19.4 |
| Average B value for main-chain non-H atoms (Å$^2$) | 17.4 |
| Average B value for side-chain non-H atoms (Å$^2$) | 19.9 |
| Average B value for waters (Å$^2$) | 27.2 |

Model statistics.

| | R.m.s. | $\sigma$ |
| --- | --- | --- |
| Bond length (Å) | 0.013 | 0.021 |
| Bond angle (°) | 1.754 | 1.942 |
| Torsion angles, period 1 (°) | 4.176 | 3.0 |
| Torsion angles, period 3 (°) | 17.488 | 15.0 |
| Chiral centre restraints (Å$^3$) | 0.121 | 0.20 |
| Plane restraint (Å) | 0.006 | 0.020 |
| VDW repulsions (Å) | 0.234 | 0.30 |
| Hydrogen bonds (Å) | 0.141 | 0.50 |

as implemented in AMoRe (Navaza, 1994) using the coordinates of cathepsin K (PDB code 1mem) as a model. Translation-function calculations carried out in both $P3_121$ and $P3_221$ unambiguously indicated the correct space group to be $P3_121$ (correlation for highest peak was 28.8 in space group $P3_221$ and 60.2 in space group $P3_121$; that for the second highest peak was 20, which is comparable to the noise level). The resulting model with one protein molecule per asymmetric unit was subsequently refined using the program REFMAC (Murshudov et al., 1997), interspersed with manual rebuilding of the model using X-AUTOFIT (Oldfield, 2001) as implemented in QUANTA (Accelrys). The initial model had a crystallographic R factor of 0.412. Water molecules were located using the X-SOLVATE module in QUANTA (Accelrys). The final model has a crystallographic R factor of 0.194 ($R_{free}$ = 0.251; Table 1) and consists of 1684 protein atoms and 173 water molecules, with 83.7% of the residues within the 'core region' and 15.8% of the residues within the 'additional allowed regions' of the Ramachandran plot (Ramakrishnan & Ramachandran, 1965) as defined by PROCHECK (Laskowski et al., 1993). No electron density representing bound substrate could be detected in the active site, which was expected as the peptide used to aid crystallography was a substrate for active cathepsin S and was not hydrolysed by the inactive enzyme. Studies on similar substrates show the mutant enzyme to be essentially inactive (Mason et al., 2001). This peptide was therefore a very weak binding ligand for cathepsin S (Cys25→Ser), resulting in very

low occupancy in the crystal lattice under the crystallogenic conditions used.

## 3. Results and discussion

The structure of cathepsin S is very similar to that of the plant protein papain, the canonical structure for this protein superfamily, and the $C^\alpha-C^\alpha$ trace follows very closely that of similar functional counterparts cathepsin L, K and H. Superposition of the main-chain atoms of 200 aligned residues in these structures onto cathepsin S Cys25→Ser results in small r.m.s. deviations: 0.69 Å for papain (PDB code 9pap; Kamphuis *et al.*, 1984), 0.34 Å for cathepsin K (PDB code 1mem; McGrath *et al.*, 1997), 0.72 Å for cathepsin H (PDB code 8pch; Gunčar *et al.*, 1998) and 0.41 Å for cathepsin L (PDB code 1cs8; Groves *et al.*, 1998). Cathepsin S forms a monomeric structure consisting of two domains. The left domain contains three helices and a hydrophobic core, whereas the right domain consists of an antiparallel $\beta$-sheet barrel enclosing a hydrophobic core with two $\alpha$-helices flanking either side of this barrel (Fig. 1). Three disulfides, two in the left domain and one in the right domain, play a role in maintaining the overall structure of the protein. The relative position of the two domains is stabilized by numerous hydrogen bonds between water molecules and the mainly polar residues lining the two walls of the cleft. In addition, the N-terminus from the left domain crosses over to the right domain and the C-terminus of the right domain in turn crosses over to the left domain, thereby anchoring the two domains. The interface between the two domains forms a deep cleft containing the catalytic triad. The catalytic His164 and the stabilizing Asp184 residue of the triad are part of the polar
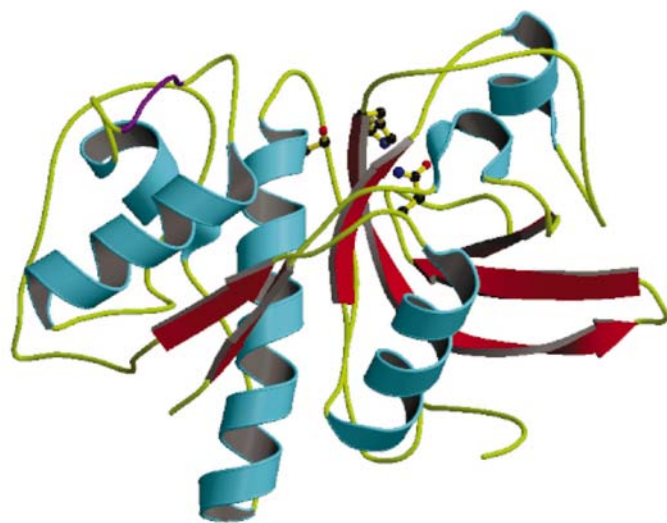
surface formed by the wall of the right domain, with the left domain contributing the mutated Ser25 at the N-terminus of the main helix in this domain. In the active site, a number of well defined water molecules were identified which are involved in an intricate hydrogen-bonding network (Fig. 2). The mutated Ser25 residue hydrogen bonds to a water molecule which in turn forms a hydrogen bond to the side-chain N atom of Gln19, which also hydrogen bonds to a second water molecule. This second water molecule forms hydrogen bonds to the side chain of Trp186 and the active-site His164, which forms a second hydrogen bond to Gln19. It is this Gln19 that forms part of the oxyanion hole, a structural feature believed to stabilize the tetrahedral intermediate in the reaction pathway. The hydrogen bond between the catalytic histidine and the Asn184 is 2.64 Å, in accordance with the distance observed in other catalytic triads. In a number of uncomplexed structures of serine proteases, this hydrogen bond was thought not to be present (Matthews *et al.*, 1977). More recent evidence suggests there may be a weak hydrogen bond (Tsukada & Blow, 1985) as present in this mutant structure. The observed network may provide a mechanism for correct orientation of the catalytic residue side chains prior to substrate hydrolysis.

As the two main catalytic residues are part of opposing walls of the catalytic cleft, it is very likely that relative movement of the walls modulates the interaction between the cysteine and histidine moieties in the active enzyme, thus
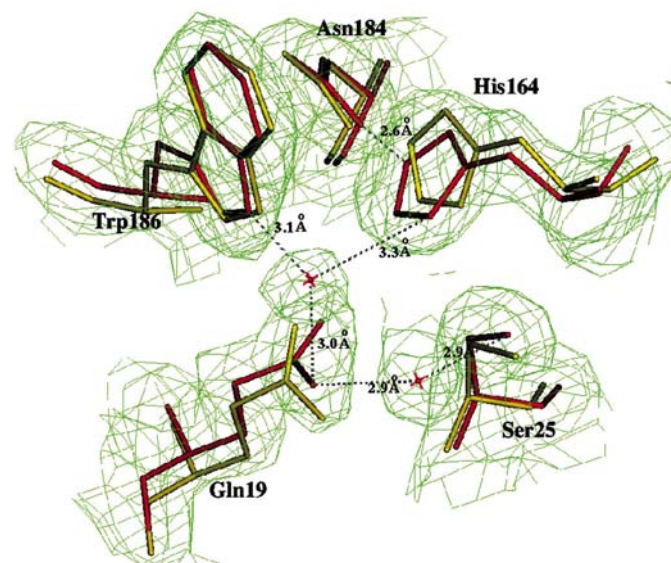


**Figure 1**
Secondary-structure ribbon model of cathepsin S with the catalytic residues Cys25→Ser, His164 and Asn187 shown in ball-and-stick representation and colour-coded by atom type. The loop running from residues 61–64, which was previously unidentified (see main text), is shown in purple. The figure was prepared using *MOLSCRIPT* (Kraulis, 1991) and *Raster3D* (Merritt & Bacon, 1997).



**Figure 2**
Superposition of the active-site residues of mutant cathepsin S (in red) and cathepsin K (in yellow). The hydrogen-bonding network for the mutant enzyme is shown. The catalytic triad (with the Ser25 mutation) is shown on the right, with three water molecules in the centre and Gln19 and Trp186 to the left. Hydrogen bonds are shown as dashed lines. The observed network may provide a mechanism for correct catalytic residue side-chain orientation prior to substrate hydrolysis. Also shown is the final maximum-likelihood-weighted electron-density map ($2F_o - F_c$), contoured at $1\sigma$ above the mean. This figure shows convincingly that the constellation of the active-site residues is essentially unchanged in the mutant.

playing a role in the catalytic mechanism. The position of the inactive mutant cathepsin S catalytic triad side chains super-imposes very closely with the catalytic triad of the active cathepsin K proteinase (Fig. 2). This observation demonstrates that it is the increased nucleophilicity of the S atom in the cathepsin K cysteine residue (compared to the O atom in the cathepsin S Cys25→Ser serine hydroxyl group) that imparts proteolytic activity in the observed structural context. The $pK_a$ of the active-site cysteine in papain-like proteinases has been measured to be 3.3 (Pinitglang *et al.*, 1997), which is far lower than that expected for serine in the equivalent position. This allows a proton to be pulled from the cysteine sulfidyl by the asparagine-polarized active-site histidine, whereas a catalytic triad aspartic acid residue is required for the histidine polarization necessary for proton abstraction from a serine residue (Tsukada & Blow, 1985).

The substrate-binding site formed between the two domains extends on either side of the catalytic residues, with three binding pockets S3, S2 and S1 for substrate residues on the amino-terminal side of the scissile bond (Schechter & Berger, 1967) and a clear binding pocket S1' at the substrate carboxy-terminal side. The previously described cathepsin S structure (McGrath *et al.*, 1998) gave a general description of the peptide-binding cleft, but did not show the cathepsin S-specific loop containing residues 61–64 (58–61 in McGrath numbering). This region of the enzyme can clearly be seen shaping the back of the S3 pocket and has important implications for the design of selective inhibitors (loop position shown in Fig. 1). For example, unlike the open cleft S3 binding region found in cathepsin K (Bossard *et al.*, 1999; Marquis, Ru,

LoCastro *et al.*, 2001; Marquis, Ru, Zeng *et al.*, 2001), cathepsin S has a small pocket which could be exploited for selectivity in drug design, for instance by the use of a small cyclic capping group at the N-terminus of a peptidomimetic inhibitor. The S3 pocket is lined by the residues Gly68 and Gly69 at the base, with Phe70, Gly62, Asn63 and Lys64 forming the sides and rear of the binding region (Fig. 3).

The relatively large open S2 pocket of cathepsin S, which also contributes to enzyme substrate selectivity, has been extensively studied (Bromme *et al.*, 1994, 1996; McGrath *et al.*, 1998) and is composed of residues Met71, Gly137, Val138, Val162, Gly165 and Phe211. This region has been shown to prefer branched hydrophobic side chains, with Gly137 appearing to provide more space relative to the alanine residue found in the equivalent position in cathepsin K and L (Fig. 3). The interactions observed in the S1 site of the covalent cathepsin S complex (McGrath *et al.*, 1998) all involve backbone atoms and this site seems to play a very minor role in the specificity of papain-like cysteine proteases.

The only obvious binding site C-terminal of the scissile bond (S1') was found to be comprised of residues Trp186, His164, Asn163 and Ala140 by McGrath *et al.* (1998). The side chain of Arg141 could not be observed in their electron-density maps, but was expected to form part of this binding site. In the current structure, the electron density for the side chain is very well defined. However, the side chain points away from the binding site, into the solvent and only forms hydrogen bonds with water molecules. The flexibility of the arginine side chain would, however, allow this residue to adopt a different conformation upon binding of a substrate, bringing it into hydrogen-bonding distance and thereby playing a role in the specificity of this enzyme. Therefore, this could be an important residue contributing to specific cleavage of MHC class II-associated invariant chain Ii by cathepsin S (Gunčar *et al.*, 1999).

## 4. Conclusions

The cathepsin S structure model described herein will be a vital tool for *in silico* docking studies directed towards the design of new therapeutic proteinase inhibitors. Moreover, the inactive mutant enzyme used will be useful in rapid cocrystallization experiments using potent non-covalent inhibitors to determine detailed binding mechanisms by X-ray crystallography. This could provide a better alternative than the native cathepsin S enzyme, where crystal generation using a covalently binding vinyl sulfone inhibitor molecule was slow and unpredictable (McGrath *et al.*, 1998).
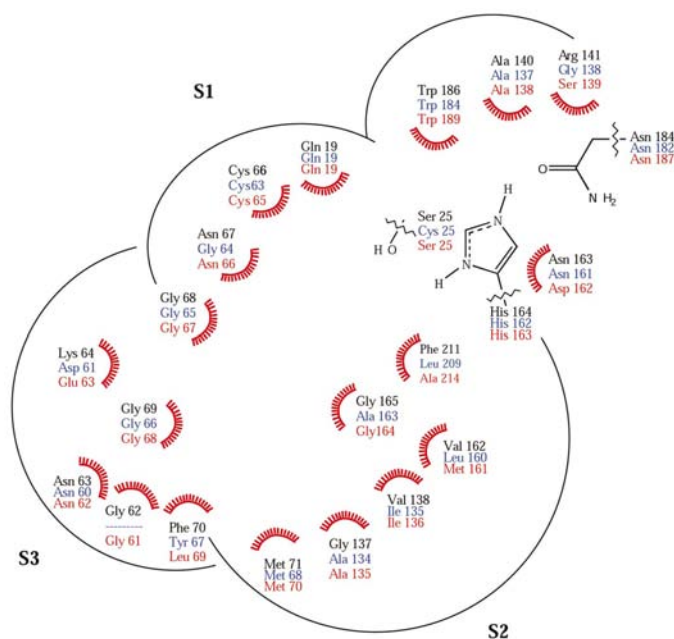
**Figure 3**
Two-dimensional representation of the residues present in the non-prime side of the cathepsin S substrate-binding site. For substrate specificity comparisons, the equivalent residues in cathepsin K (PDB code 1mem) and cathepsin L (PDB code 1cs8) are shown in blue and red, respectively.

## References

Bossard, M. J., Tomaszek, T. A., Levy, M. A., Ijames, C. F., Huddleston, M. J., Briand, J., Thompson, S., Halpert, S., Veber, D. F., Carr, S. A., Meek, T. D. & Tew, D. G. (1999). *Biochemistry*, **38**, 15893–15902.

Bromme, D., Bonneau, P. R., Lachance, P. & Storer, A. C. (1994). *J. Biol. Chem.* **269**, 30238–30242.

Bromme, D., Klaus, J. L., Okamoto, K., Rasnick, D. & Palmer, J. T. (1996). *Biochem. J.* **315**, 85–89.

Collaborative Computational Project, Number 4 (1994). *Acta Cryst.* **D50**, 760–763.

Cresswell, P. (1996). *Cell*, **84**, 505–507.

Germain, R. N. & Margulies, D. H. (1993). *Annu. Rev. Immunol.* **11**, 403–450.

Gowen, M., Lazner, F., Dodds, R., Kapadia, R., Feild, J., Tavaria, M., Bertoncello, I., Drake, F., Zavarselk, S., Tellis, I., Hertzog, P., Debouck, C. & Kola, I. (1999). *J. Bone Miner. Res.* **14**, 1654–1663.

Groves, M. R., Coulombe, R., Jenkins, J. & Cygler, M. (1998). *Proteins*, **32**, 504–514.

Gunčar, G., Podobnik, M., Pungercar, J., Strukelj, B., Turk, V. & Turk, D. (1998). *Structure*, **6**, 51–61.

Gunčar, G., Pungerčič, G., Klemenčič, I., Turk, V. & Turk, D. (1999). *EMBO J.* **18**, 793–803.

Hofbauer, L. C. & Heufelder, A. E. (1999). *Eur. J. Endocrinol.* **140**, 376–377.

Kamphuis, I. G., Kalk, K. H., Swarte, M. B. A. & Drenth, J. (1984). *J. Mol. Biol.* **179**, 233–256.

Kirschke, H., Schmidt, I. & Wiederanders, B. (1986). *Biochem. J.* **240**, 455–459.

Kirschke, H., Wiederanders, B., Bromme, D. & Rinne, A. (1989). *Biochem. J.* **264**, 467–473.

Kraulis, P. J. (1991). *J. Appl. Cryst.* **24**, 946–950.

Laskowski, R. A., MacArthur, M. W., Moss, D. S. & Thornton, J. M. (1993). *J. Appl. Cryst.* **26**, 283–291.

McGrath, M. E., Klaus, J. L., Barnes, M. G. & Bromme, D. (1997). *Nature Struct. Biol.* **4** 105–109.

McGrath, M. E., Palmer, J. T., Bromme, D. & Somoza, J. R. (1998). *Protein Sci.* **7**, 1294–302.

Marquis, R. W., Ru, Y., LoCastro, S. M. *et al.* (2001). *J. Med. Chem.* **44**, 1380–1395.

Marquis, R. W., Ru, Y., Zeng, J., Trout, R. E., LoCastro, S. M., Gribble, A. D., Witherington, J., Fenwick, A. E., Garnier, B., Tomaszek, T., Tew, D., Hemling, M. E., Quinn, C. J., Smith, W. W., Zhao, B., McQueney, M. S., Janson, C. A., D'Alessio, K. & Veber, D. F. (2001). *J. Med. Chem.* **44**, 725–736.

Mason, C. S., Lamers, M. B. A. C., Henderson, I. M. J., Monk, T. & Williams, D. H. (2001). *Protein Expr. Purif.* **23**, 45–54.

Matthews, B. W. (1968). *J. Mol. Biol.* **33**, 491–497.

Matthews, D. A., Alden, R. A., Birktoft, J. J., Freer, T. & Kraut, J. (1977). *J. Biol. Chem.* **252**, 8875–8883.

Merritt, E. A. & Bacon, D. J. (1997). *Methods Enzymol.* **277**, 505–524.

Murshudov, G. N., Vagin, A. A. & Dodson, E. J. (1997). *Acta Cryst.* **D53**, 240–255.

Nakagawa, T. Y., Brissette, W. H., Lira, P. D., Griffiths, R. J., Petrushova, N., Stock, J., McNeish, J. D., Eastman, S. E., Howard, E. D., Clarke, S. R., Rosloniec, E. F., Elliott, E. A. & Rudensky, A. Y. (1999). *Immunity*, **10**, 207–217.

Nakagawa, T., Roth, W., Wong, P., Nelson, A., Farr, A., Deussing, J., Villadangos, J. A., Ploegh, H., Peters, C. & Rudensky, A. Y. (1998). *Science*, **280**, 450–453.

Navaza, J. (1994). *Acta Cryst.* **A50**, 157–163.

Newcomb, J. R. & Cresswell, P. (1993). *J. Immunol.* **150**, 499–507.

Oldfield, T. J. (2001). *Acta Cryst.* **D57**, 82–94.

Otwinowski, Z. & Minor, W. (1997). *Methods Enzymol.* **276**, 307–326.

Pinitglang, S., Watts, A. B., Patel, M., Reid, J. D., Noble, M. A., Gul, S., Bokth, A., Naeem, A., Patel, H., Thomas, E. W., Sreedharan, S. K., Verma, C. & Brocklehurst, K. (1997). *Biochemistry*, **36**, 9968–9982.

Qian, F., Chan, S. J., Gong, Q. M., Bajkowski, A. S., Steiner, D. F. & Frankfater, A. (1991). *Biomed. Biochim. Acta*, **50**, 531–540.

Ramakrishnan, C. & Ramachandran, G. N. (1965). *Biophys. J.* **5**, 909–933.

Riese, R. J., Mitchell, R. N., Villadangos, J. A., Shi, G. P., Palmer, J. T., Karp, E. R., De Sanctis, G. T., Ploegh, H. L. & Chapman, H. A. (1998). *J. Clin. Invest.* **101**, 2351–2363.

Riese, R. J., Wolf, P. R., Bromme, D., Natkin, L. R., Villadangos, J. A., Ploegh, H. L. & Chapman, H. A. (1996). *Immunity*, **4**, 357–366.

Roche, P. A. & Cresswell, P. (1991). *Proc. Natl Acad. Sci. USA*, **88**, 3150–3154.

Saftig, P., Hunziker, E., Wehmeyer, O., Jones, S., Boyde, A., Rommerskirch, W., Moritz, J. D., Schu, P. & von Figura, K. (1998). *Proc. Natl Acad. Sci. USA*, **95**, 13453–13458.

Schechter, I. & Berger, A. (1967). *Biochem. Biophys. Res. Commun.* **27**, 157–62.

Shi, G. P., Villadangos, J. A., Dranoff, G., Small, C., Gu, L., Haley, K. J., Riese, R., Ploegh, H. L. & Chapman, H. A. (1999). *Immunity*, **10**, 197–206.

Shi, G. P., Webb, A. C., Foster, K. E., Knoll, J. H., Lemere, C. A., Munger, J. S. & Chapman, H. A. (1994). *J. Biol. Chem.* **269**, 11530–11536.

Sumpter, J. A., Compadre, R. L., Bhuvaneswaran, C. & Compadre, C. M. (1997). *Biomed. Health Res.* **13**, 22–27.

Tsukada, H. & Blow, D. M. (1985). *J. Mol. Biol.* **184**, 703–711.

Turnsek, T., Kregar, I. & Lebez, D. (1975). *Biochim. Biophys. Acta*, **403**, 514–520.

Vernet, T., Tessier, D. C., Richardson, C., Laliberte, F., Khouri, H. E., Bell, A. W., Storer, A. C. & Thomas, D. Y. (1990). *J. Biol. Chem.* **265**, 16661–16666.